

Synthesis, structure and luminescence of novel 2D co-crystals based on asymmetric 5-substituted pyrimidines and isophthalic acid: Alternate arrangement and π - π interactions

Xian-Ping Dai, Gui-Ge Hou*, Ju-Feng Sun, Dong Lin, Jing-Tian Han*

School of Pharmacy, Binzhou Medical University, Yantai, Shandong 264003, PR China

HIGHLIGHTS

- ▶ Two novel co-crystals (**A**) (isophthalic acid) (**1**) and (**B**) (isophthalic acid) (**2**) were generated and characterized.
- ▶ The crystal packing in **1**, **2** generated infinite zigzag chains, further 2D planar networks.
- ▶ Emission intensities of **1**, **2** distinctly decrease compared with 5-substituted pyrimidines.
- ▶ The luminescent property is dependent on the intermolecular – ABAB – alternate arrangement and π - π contacting characteristic.

ARTICLE INFO

Article history:

Received 31 July 2012

Received in revised form 13 November 2012

Accepted 19 November 2012

Available online 28 November 2012

Keywords:

Co-crystals

Asymmetric building blocks

Crystal structures

Luminescence properties

ABSTRACT

Two novel organic co-crystals (**A**) (isophthalic acid) (**1**) and (**B**) (isophthalic acid) (**2**), were generated based on asymmetric building blocks 5-(4-pyridyl)pyrimidine (**A**) and 5-(4-(1-imidazolyl)phenyl)pyrimidine (**B**) with isophthalic acid, respectively. The building blocks interlinked with isophthalic acid through intermolecular H-bonding interactions to generate infinite chains, which further extended 2D planar networks. In addition, the luminescent properties of **A**, **B** and **1**, **2** were investigated primarily in the solid state. Compared with the free building blocks, the emission maxima of **1** and **2** have not been changed, but emission intensities of **1** and **2** have decreased. The structure–property relationship indicates the luminescent property is dependent on the intermolecular – ABAB – alternate arrangement and the intermolecular π - π contacting characteristic. By incorporation of conformers into the co-crystals, the results display more interesting tunability of the emission intensities of the building modules in this study.

© 2012 Elsevier B.V. All rights reserved.

1. Introduction

Due to their strength and directionality, hydrogen bonds have been widely used in the construction of supramolecular aggregation [1–5]. During the past few decades, Etter's set of rules for hydrogen bonding interaction in organic crystals [6], Desiraju's concept of 'supramolecular synthons' [7] and Zaworotko's definition of "co-crystal" [8] have been brought forward. Co-crystals are able to offer the aggregation to modify the physical properties of subset involved without changing the compound structure. Some of them have shown encouraging potential in pharmaceutical application and solid-state organic synthesis [9–12]. However, investigation of co-crystals as luminescent materials is extremely rare [13–15]. In terms of fundamental studies and practical applications, the ability to tune and control the luminescent color or

intensity of an organic material is important to achieve multi-color materials or intensity-tunable fluorescent materials, and ultimately meet the requirement for next generation light-emitting materials [16]. To obtain potential organic co-crystals with outstanding luminescent properties is a challenge for scientists. Recent advances in organic co-crystals have indicated that the intermolecular interactions and molecular stacking patterns in the solid state play a key role in the observed bulk luminescent characteristics. Co-crystals are molecular solids composed of at least two types of neutral chemical species. In organic co-crystals, incorporation of different conformers with the different functional groups and orientations may profoundly influence the structural assemblies and luminescent properties because of their different hydrogen bonding capability and steric/electronic effect. Therefore, the exploration of novel and patentable co-crystals with luminescent properties is very significant.

Previously, some symmetric pyrimidine derivatives, such as 5,5'-dipyrimidine, 1,2-bis(5'-pyrimidyl)ethyne, were occasionally used as "linear" building blocks in supramolecular chemistry and

* Corresponding authors.

E-mail addresses: guigeou@163.com (G.-G. Hou), hanjingtian002@163.com (J.-T. Han).

the construction of co-crystals [17–19]. However, the hydrogen bonding driven organic co-crystals based on asymmetric pyrimidine derivatives have not been received much attention [20]. Thus the inclusion of different functional groups, such as pyrimidine, pyridine and imidazole, may lead to the different and patentable co-crystals with versatile structures and potential properties.

In addition, some aromatic carboxylic acids as hydrogen-bond donors have been selected to investigate hydrogen-bond topology and dimensionality [21,22]. In this study, we report two novel co-crystals, namely [(A) (isophthalic acid)] (**1**) and [(B) (isophthalic acid)] (**2**) based on **A**, **B** with isophthalic acid.

2. Experimental

2.1. Materials and methods

A and **B** was prepared according to a literature [23]. Infrared (IR) samples were prepared as KBr pellets, and spectra were obtained in the 400–4000 cm^{-1} range using a Bruker tensor-27 FTIR spectrometer. ^1H NMR data were collected using a Bruker Avance-400 spectrometer. Chemical shifts were reported in δ relative to TMS. Elemental analyses were performed on a Perkin–Elmer Model 240c analyzer. All fluorescence measurements were carried out on a Cary Eclipse Spectrofluorimeter (Varian, Australia) equipped with a xenon lamp and quartz carrier at room temperature. XRD pattern were obtained on a Rigaku D/Max-rB X-ray powder diffraction (XRD) with Cu $K\alpha$ radiation ($\lambda = 1.5405$ & Aring). The yields were calculated from the crystalline samples after removal of the solvent under vacuum and the molar amounts initially introduced.

2.2. Preparation of co-crystals 1–2

A CH_2Cl_2 and CH_3CN solution (10 mL, 1:1, v/v) of **A** (15.7 mg, 0.1 mmol) with isophthalic acid (16.6 mg, 0.1 mmol) or **B** (22.2 mg, 0.1 mmol) with isophthalic acid (16.6 mg, 0.1 mmol), was kept at room temperature. Upon slow evaporation of the solvent about 5 days, colorless crystals **1–2** were obtained, respectively.

2.2.1. Co-crystal 1

Yield: 80%. IR (KBr Pellet cm^{-1}): 3076(s), 2814(s), 2457(br), 1880(br), 1705(s), 1603(s), 1575(s), 1415(s), 1281(s), 1254(s), 1188(s), 1070(s), 999(m), 827(s), 725(s). ^1H NMR (400 MHz, DMSO, 25 °C, TMS, ppm): 13.26 (s, 2H, –COOH), 9.29 (d, 3H, – $\text{C}_4\text{H}_3\text{N}_2$), 8.74 (d, 2H, – $\text{C}_5\text{H}_4\text{N}$), 8.48 (s, 1H, – C_6H_4), 8.17 (d, 2H, – C_6H_4), 7.89 (d, 2H, – $\text{C}_5\text{H}_4\text{N}$), 7.64 (m, 1H, – C_6H_4). Elemental analysis (%) calcd. for $\text{C}_{17}\text{H}_{13}\text{N}_3\text{O}_4$ (323.30): C 63.15, H 4.05, N 12.99; Found: C 63.43, H 4.01, N 12.78.

2.2.2. Co-crystal 2

Yield: 85%. IR (KBr Pellet cm^{-1}): 3133(s), 2493(br), 1891(br), 1704(s), 1613(m), 1529(m), 1402(s), 1322(s), 1280(s), 1118(s), 1056(s), 828(s), 760(s), 733(m), 683(m). ^1H NMR (400 MHz, DMSO, 25 °C, TMS, ppm): 13.32 (s, 2H, –COOH), 9.22 (d, 3H, – $\text{C}_4\text{H}_3\text{N}_2$), 8.49 (s, 1H, – C_6H_4), 8.40 (s, 1H, – $\text{C}_3\text{H}_3\text{N}_2$), 8.18 (d, 2H, – C_6H_4), 7.98 (d, 2H, – C_6H_4), 7.87 (m, 1H, – $\text{C}_3\text{H}_3\text{N}_2$, 2H, – C_6H_4), 7.66 (m, 1H, – C_6H_4), 7.16 (s, 1H, – $\text{C}_3\text{H}_3\text{N}_2$). Elemental analysis (%) calcd. for $\text{C}_{21}\text{H}_{16}\text{N}_4\text{O}_4$ (388.37): C 64.94, H 4.15, N 14.42; Found: C 64.56, H 4.34, N 14.67.

2.3. Single-crystal structure determination

Suitable single crystals of **1–2** were selected and mounted in air onto thin glass fibers. X-ray intensity data of **1–2** were measured at 293 K on a Bruker SMART APEX CCD-based diffractometer (Mo $K\alpha$

Table 1
Crystallographic data for **1–2**.

Compound	1	2
Empirical formula	($\text{C}_9\text{H}_7\text{N}_3$)($\text{C}_8\text{H}_6\text{O}_4$)	($\text{C}_{13}\text{H}_{10}\text{N}_4$)($\text{C}_8\text{H}_6\text{O}_4$)
CCDC Deposit no.	875334	855281
Color/shape	Yellow, block	Colorless, plan
Formula weight	323.30	388.38
Temperature (K)	298(2)	298(2)
Crystal system	Triclinic	Monoclinic
Space group	$P1$	$P2_1/c$
<i>a</i> (Å)	6.6918(16)	10.5685(19)
<i>b</i> (Å)	7.4746(18)	13.080(2)
<i>c</i> (Å)	16.150(4)	13.537(2)
α (°)	80.283(4)	90
β (°)	88.014(3)	104.649(3)
γ (°)	68.827(3)	90
Volume (Å ³)	742.2(3)	1810.5(6)
<i>Z</i>	2	4
ρ calc. (g/cm ³)	1.447	1.425
μ (Mo $K\alpha$) (mm ⁻¹)	0.106	0.102
<i>F</i> (000)	336	808
Limiting indices	$-7 \leq h \leq 8$, $-19 \leq l \leq 19$	$-12 \leq h \leq 10$, $-15 \leq k \leq 15$, $-15 \leq l \leq 16$
Crystal size (mm)	0.30 × 0.14 × 0.06	0.30 × 0.22 × 0.08
Theta range for data collection (°)	2.56–25.49	1.99–25.50
Completeness to θ	98.2%	99.7%
Reflections collected	3916	9348
Independent reflections	2705 [$R(\text{int}) = 0.0274$]	3357 [$R(\text{int}) = 0.0472$]
Data/restraints/parameters	2705/0/219	3357/0/263
Goodness-of-fit on F^2	1.061	1.106
Final <i>R</i> indices	$R_1 = 0.0524$, $wR_2 = 0.1326$	$R_1 = 0.0725$, $wR_2 = 0.1456$
$[I > 2\sigma(I)]$		
<i>R</i> indices (all data)	$R_1 = 0.0634$, $wR_2 = 0.1419$	$R_1 = 0.1148$, $wR_2 = 0.1628$
Largest diff. peak and hole $e\text{-}\text{Å}^{-3}$	0.189 and –0.247	0.182 and –0.230

$$^a R_1 = \sum ||F_o| - |F_c|| / \sum |F_o|. wR_2 = \{\sum [w(F_o^2 - F_c^2)^2] / \sum [w(F_o^2)^2]\}^{1/2}.$$

radiation, $\lambda = 0.71073$ Å). The raw frame data for **1–2** were integrated into SHELX-format reflection files and corrected for Lorentz and polarization effects using SAINT [24]. None of the crystals showed evidence of crystal decay during data collection. All structures were solved by a combination of direct methods and difference Fourier syntheses and refined against F^2 by the full-matrix least squares technique. Crystal data, data collection parameters, and refinement statistics for **1**, **2** are listed in Table 1. Relevant hydrogen-bonding geometries for **1–2** are shown in Table 2.

3. Results and discussion

3.1. Structural analysis

3.1.1. Co-crystal [(A) (isophthalic acid)] (**1**)

Single-crystal structure reveals that co-crystal **1** exhibits an 1:1 stoichiometric ratio of components, corresponding to the formula (A) (isophthalic acid) (Fig. 1). In **1**, the desired O–H \cdots N (O(2)–H(2A) \cdots N(1) and O(3)–H(3) \cdots N(2)) hydrogen bonding systems are formed between **A** and isophthalic acid into a zigzag chain with a $C_2^2(16)$ motif extended along the crystallographic [01–1] axes (Fig. 2a). In **A** molecule, pyrimidyl and pyridyl groups are not fully coplanar, and the dihedral angle between them is approximately 23.8°.

In the solid state, adjacent chains are connected to each other through weak interchain C(9)–H(9) \cdots O(4) [25,26] hydrogen bonds into a H-bonding-driven parquet-like network extended in the crystallographic *ac* plane (Fig. 2b). The parquet-like grid displays

Table 2
Relevant hydrogen-bonding geometries (Å, °) found in **1–2**.

D–H...A	<i>d</i> (D–H)	<i>d</i> (H...A)	<i>d</i> (D...A)	∠(DHA)	Symmetry code
1					
O(2)–H(2A)...N(1) ⁱ	0.82	1.83	2.650(2)	176.9	i: – <i>x</i> , – <i>y</i> , – <i>z</i> + 1
O(3)–H(3)...N(2) ⁱⁱ	0.82	1.88	2.702(2)	178.8	ii: – <i>x</i> , – <i>y</i> + 1, – <i>z</i>
C(9) ⁱⁱⁱ –H(9) ⁱⁱⁱ ...O(4)	0.93	2.36	3.209(2)	150.8	iii: – <i>x</i> + 1, – <i>y</i> + 1, – <i>z</i>
2					
O(1)–H(1A)...N(1) ⁱ	0.82	1.78	2.602(3)	175.4	i: <i>x</i> + 1, – <i>y</i> + 3/2, <i>z</i> + 1/2
O(4)–H(4)...N(3) ⁱⁱ	0.82	1.86	2.678(3)	173.5	ii: <i>x</i> – 1, <i>y</i> , <i>z</i>
C(20) ⁱⁱⁱ –H(20) ⁱⁱⁱ ...O(2) ⁱⁱⁱ	0.93	2.49	3.279(3)	142.4	iii: – <i>x</i> + 2, – <i>y</i> + 1, – <i>z</i> + 1
C(2) ^{iv} –H(2) ^{iv} ...O(1)	0.93	2.38	3.298(3)	168.2	iv: – <i>x</i> + 1, <i>y</i> + 1/2, – <i>z</i> + 1/2
C(3) ^{iv} –H(3) ^{iv} ...O(3)	0.93	2.41	3.328(3)	166.5	iv: – <i>x</i> + 1, <i>y</i> + 1/2, – <i>z</i> + 1/2
C(8) ^{iv} –H(8) ^{iv} ...N(4) ⁱⁱ	0.93	2.72	3.521(4)	144.6	ii: <i>x</i> – 1, <i>y</i> , <i>z</i> iv: – <i>x</i> + 1, <i>y</i> + 1/2, – <i>z</i> + 1/2

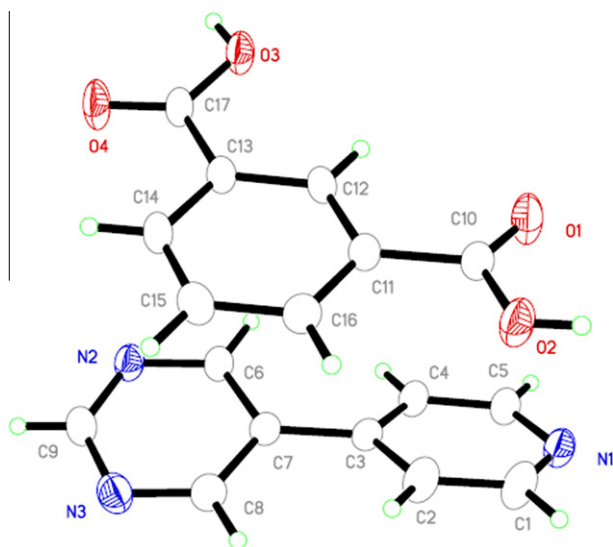


Fig. 1. The ORTEP figure of **1** (displacement ellipsoids with 30% probability).

an $R_6^6(40)$ motif. Relevant hydrogen-bonding geometries are given in Table 2. In this network, the isophthalic acid plane is basically parallel from H-bond linked pyrimidyl groups (the dihedral angle approximately 2.3°), while it is angulate with H-bond linked pyridyl group (the dihedral angle approximately 22.0°).

3.1.2. Co-crystal [(**B**) (isophthalic acid)] (**2**)

One of the important issues in determining the dimensions of porous frameworks is the scale of the building blocks. In principle, the lengthening conjugated spacers used, the larger pore dimensions would be obtained. To achieve novel frameworks with versatile structures and potential properties, we selected building block **B** with longer dimension, which has asymmetric pyrimidine and imidazole groups.

As shown in Fig. 3, co-crystal **2** consists of one crystallographically independent **B** and one isophthalic acid molecule, corresponding to the formula (**B**) (isophthalic acid). A similar zigzag chain with **1** along the crystallographic *a* axes can be found in Fig. 4a. Isophthalic acid links two **B** molecules to generate a zigzag chain through O–H...N (O(1)–H(1A)...N(1) and O(4)–H(4)...N(3))

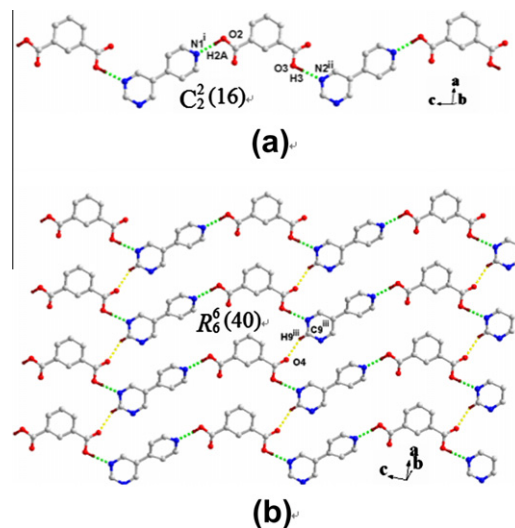


Fig. 2. (a) The $C_2^2(16)$ zigzag chain extended along the crystallographic [01–1] axes. (b) The H-bonded network with $R_6^6(40)$ grids in **1**. (Symmetry code: i: –*x*, –*y*, –*z* + 1; ii: –*x*, –*y* + 1, –*z*; iii: –*x* + 1, –*y* + 1, –*z*.)

hydrogen bonds. This chain exhibits a $C_2^2(19)$ motif. However, obvious structural difference of the 2D hydrogen-bonding sheet along the crystallographic *ab* plane from robust **1** can be found in **2** (Fig. 4b). Complicated hydrogen bonding motifs are shown in Fig. 4b. Two isophthalic acids connect each other through two groups of C(20)–H(20)...O(2) bonds to generate an $R_2^2(10)$ motif. Two hydroxy groups of two isophthalic acids participate in an intermolecular C(2)–H(2)...O(1) and O(1)–H(1A)...N(1) hydrogen bonds with the imidazole groups to form an $R_4^4(10)$ ring. And $R_4^4(28)$ grids are formed in the 2D sheet, lightly smaller than the $R_6^6(40)$ grids of **1**. In addition, the same isophthalic acid links an imidazole group to an $R_2^2(11)$ motif. Therefore, isophthalic acid and imidazole plane are almost coplanar, proved by the dihedral angle 6.6° between them. In the 2D sheet, an $R_3^3(14)$ motif is formed through intermolecular hydrogen bonds. So isophthalic acid and pyrimidine group are almost coplanar (the dihedral angle ca. 4.4°). The auxiliary O–H...N and C–H...O interactions may hold out the rigidity of such hydrogen-bonding motifs and thus result in the coplanarity of **B** and isophthalic acid. Detailed hydrogen bonds are shown in Fig. 4 and relevant hydrogen-bonding geometries are given in Table 2. For **B**, the asymmetric hydrogen-bonding interactions of both terminal groups influence its coplanarity, which can be confirmed by the dihedral angles from imidazole and pyrimidine compared with central phenyl ring, 20.8° and 21.2°, respectively. Due to the longer dimension of **B**, relatively

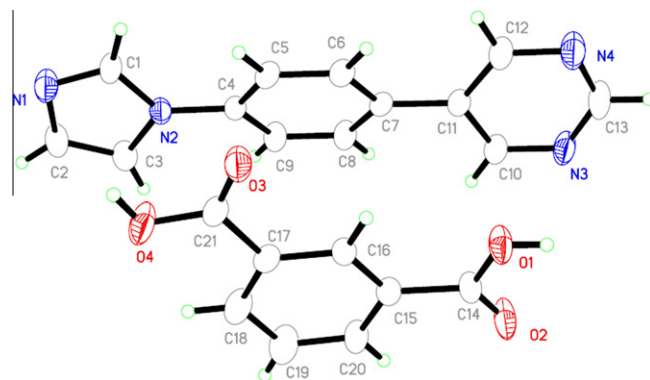


Fig. 3. The ORTEP figure of **2** (displacement ellipsoids with 30% probability).

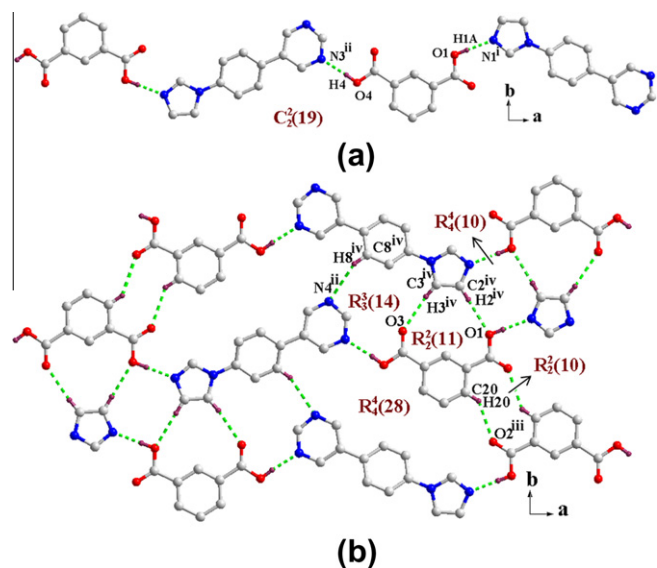


Fig. 4. (a) The $C_2^2(19)$ zigzag chain along the crystallographic a axes in **2**. (b) The H-bonded network of **2**. (Symmetry code: i: $x+1, -y+3/2, z+1/2$; ii: $x-1, y, z$; iii: $-x+2, -y+1, -z+1$; iv: $-x+1, y+1/2, -z+1/2$.)

complicated hydrogen bonding systems are build in **2** but not the simple parquet-like network in **1**. Whereas, these hydrogen-bonding self-assembly systems can provide an excellent advantage to study the interesting luminescent properties.

As described in the experimental section, co-crystals **1** and **2** were prepared by direct assembly in CH_2Cl_2 and CH_3CN solution under the ambient condition and crystallization via solvent evaporation. 1H NMR spectra of the solution were collected on crystalline samples of **1** and **2**. 1H NMR spectra indicated that the chemical shift values were completely identical to that of the original materials [23], indicating the formation of the neutral and discrete molecules in solution. Both **A** and **B** form co-crystals in 1:1 stoichiometric ratio with isophthalic acid, corresponding to their molecular formulas obtained from crystal analysis. As a matter of fact, the phase purity of the bulk crystalline solid was well confirmed by powder X-ray diffraction (PXRD) technique. As shown in Fig. 5, the PXRD patterns of **1** and **2** obtained from the bulk crystalline solid at room temperature are basically identical to those of simulated ones based on single-crystal X-ray diffraction data.

3.2. Luminescent properties of **A**, **B**, **1** and **2**

The solid-state emission spectra of co-crystals **1** and **2** with approximate 25 mg crystalline samples, respectively, were investigated primarily at room temperature. Fig. 6 presents the comparison of the emission spectra of co-crystal **1** with **A** and **2** with **B**, respectively. In the solid state, co-crystal **1** exhibits emission maximum at ca. 487 nm upon excitation at $\lambda = 389$ nm. Compared to **A** [23] and **1**, the emission maxima of **B** [23] and **2** are clearly red-shifted and **2** exhibits emission maximum at ca. 510 nm upon excitation at $\lambda = 394$ nm. The lengthening conjugated spacer by insertion of an additional phenyl space in **B** may result in the increasing electron-transporting effect of extended conjugated systems along with the red-shifted color in **B** and **2**. Compared to emission maxima of **A** (484 nm) or **B** (506 nm) [23], the emission maxima are not any change, but emission intensities of **1** and **2** distinctly decrease.

On the one hand, the – ABAB – alternate arranging disposition between building modules and isophthalic acids in co-crystals badly influenced the intermolecular electron-transport in spite of

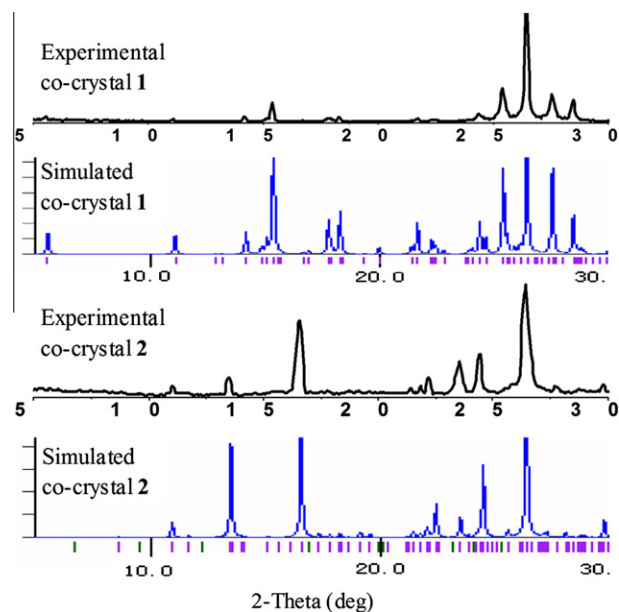


Fig. 5. The PXRD patterns (black lines) obtained from the as-synthesized solids of **1** and **2** and the simulated PXRD patterns (blue lines) from single crystals of **1** and **2**. (For interpretation of the references to color in this figure legend, the reader is referred to the web version of this article.)

the hydrogen bonding interactions. In **1**, pyrimidyl and pyridyl groups of **A** molecule are not fully coplanar, proved by the dihedral angle approximately 23.8° . Isophthalic acid plane is basically angulate with H-bond linked pyridyl group (the dihedral angle approximately 22.0°). Therefore, after introduction of the cofomer, electron transfer is obviously affected herein due to intramolecular and intermolecular distortion. So, **1** displays distinctly weak emission intensity than **A** in the solid state. The similar – ABAB – alternate arranging disposition can be found in **2**. However, the molecular conformations and the planar characteristic of 2D hydrogen-bonding sheet could even more affect the emission property of **2** in the solid state. In other words, the complex hydrogen bonding characteristic affects the intramolecular and intermolecular coplanar level as well as the mutual rigidification of components. As described above, several hydrogen-bonding motifs, such as $C_2^2(19)$, $R_2^2(10)$ and $R_4^4(10)$ motifs hold out the rigidity of such hydrogen-bonding network and thus result in the coplanarity of **B** and isophthalic acid. The isophthalic acid planes are almost coplanar from imidazole and pyrimidine, respectively, proved by the dihedral angles ca. 6.6° and ca. 4.4° . However, compared with middle phenyl group in **B** molecule, larger dihedral angles are formed from imidazole and pyrimidine, respectively, ca. 20.8° and ca. 21.2° . Actually, **2** displays distinctly weak emission intensity than **B** in the solid state because of the introduction of isophthalic acid. Therefore, by introduction of the cofomers, the arranging disposition and coplanarity of components within the original co-crystals have been changed at different levels, and thus the solid-state luminescent properties can be further tuned.

On the other hand, their different intermolecular π – π contacting characteristic in the co-crystals can influence π and π^* electron-transport. It is well known that the intermolecular π – π interaction in the organic molecular packing structure is the critical factor that determines the solid state emission colours and emission intensities [27]. The parallel stack and the centroid–centroid distances of the two building modules through the intermolecular π – π interactions are listed in Fig. 7. These building module molecules are parallel packing in – ABAB – stacking fashion from isophthalic acids. The centroid–centroid distances

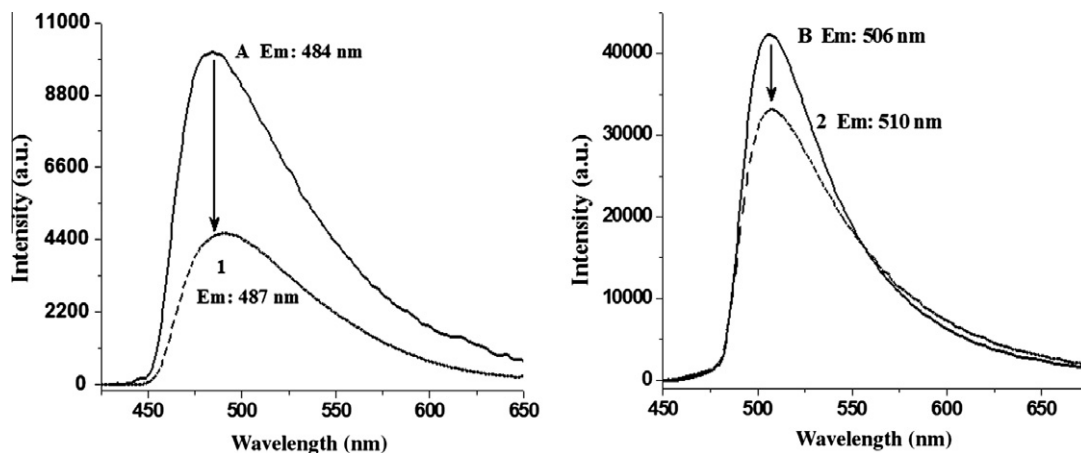


Fig. 6. Solid-state photoinduced emission spectra of **A** with **1** (excitation 389 nm) and **B** with **2** (excitation 394 nm) at room temperature.

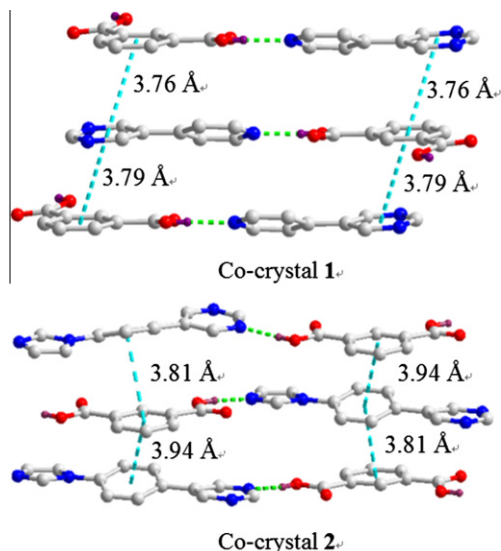


Fig. 7. View of the characteristic of intermolecular π - π stacking interactions in **1** and **2**, respectively.

are ca. 3.76 Å, 3.79 Å in **1** and 3.81 Å, 3.94 Å in **2**. The weak π - π stacking interactions enhance the rigidification of π -conjugated systems for the realization of π and π^* electron-transport. Whereas, the separated effect from isophthalic acids in - ABAB - stacking chain may seriously affect π and π^* electron-transport between building modules. Actually, the emission intensities of the co-crystals distinctly decrease.

Except for the different molecular arranging disposition and the different intermolecular π - π contacting characteristic, other factors (such as the different molecular conformations, hydrogen bonding interactions and particle size of crystalline samples) could also affect the emission properties of co-crystals in the solid state [28]. Although we cannot give further explanations for the relationship between the solid-state emission properties and the molecular packing, conformations, cofomers, it is clear that the luminescent properties of co-crystals are basically related to the introduction of the cofomers. The introduction of the cofomers can change the geometric arrangement of components in the co-crystal, which present new insight into the structure-property relationship of these co-crystal systems. Notably, they display more interesting tunability of the emission intensity of the building modules by the incorporation of cofomers into the

H-bonding-driven co-crystals compared to the pure building modules. The strategy provides a facile way to design and develop new types of solid fluorescent materials.

4. Conclusions

In this study, two novel 2D organic co-crystals were generated based on two asymmetric 5-substituted pyrimidines **A** and **B** with isophthalic acid, respectively. **A** and **B** with different functional groups, such as pyrimidine, pyridine and imidazole, provide great advantage on the hydrogen-bonding self-assembly system. In other words, the asymmetric structures, the different functional groups and the different dimensions of the building modules can profoundly affect the hydrogen bonding supramolecular recognition and further crystal packing. At the same time, isophthalic acid as hydrogen-bond donor also shows its particular advantage in investigating hydrogen-bond topology and dimensionality. As described above, the asymmetric building modules **A** and **B** interlink with isophthalic acid through intermolecular H-bonding interactions to generate infinite chains, and further extend 2D planar networks in **1**, **2**.

Both co-crystals display interesting luminescence in the solid state. The emission intensities of the asymmetric building modules are significantly influenced by their incorporation of conformers into the co-crystals. The structure-property relationship of these co-crystal systems is summarized, which indicates that the solid state emission intensity is dependent on the molecular arranging disposition and the intermolecular π - π contacting characteristic. The results also display more interesting tunability of the emission intensity of the building modules by the incorporation of conformers into the H-bonding-driven co-crystals. It might have potential applications for the organic crystal engineering to construct patentable crystals with interesting luminescent properties.

Acknowledgments

We are grateful for financial support from the National Natural Science Foundation of China (Grant Nos. 30970298, 31170320), the Foundation of Shandong province (No. J11LF27), the Foundation of Yantai City (No. 2011076) and the Scientific Foundation of Binzhou Medical University (No. BY2011KYQD08).

Appendix A. Supplementary material

CCDC 875334 (**1**), 855281 (**2**) contain the supplementary crystallographic data for this paper. Copies of the data can be obtained free of charge on application to CCDC, 12 Union Road, Cambridge

CB2 1EZ, UK (fax: +44 1223 336 033; e-mail: deposit@ccdc.cam.ac.uk). Supplementary data associated with this article can be found, in the online version, at <http://dx.doi.org/10.1016/j.molstruc.2012.11.039>.

References

- [1] A. Nangia, *Acc. Chem. Res.* 41 (2008) 595.
- [2] B. Moulton, M.J. Zaworotko, *Chem. Rev.* 101 (2001) 1629.
- [3] J.J. Jang, L. Li, T. Yang, D.B. Kuang, W. Wang, C.Y. Su, *Chem. Commun.* (2009) 2387.
- [4] P.R. Schreiner, *Chem. Soc. Rev.* 32 (2003) 289.
- [5] R.M. McKinlay, J.L. Atwood, *Angew. Chem. Int. Ed.* 46 (2007) 2394.
- [6] M.C. Etter, *Acc. Chem. Res.* 23 (1990) 120.
- [7] G.R. Desiraju, *Angew. Chem. Int. Ed. Engl.* 34 (1995) 2311.
- [8] M.J. Zaworotko, *Cryst. Growth Des.* 7 (2007) 4.
- [9] M.L. Cheney, M.J. Zaworotko, S. Beaton, R.D. Singer, *J. Chem. Educ.* 85 (2008) 1649.
- [10] D. Ajami, J. Jr Rebek, *J. Am. Chem. Soc.* 128 (2006) 5314.
- [11] M.K. Stanton, A. Bak, *Cryst. Growth Des.* 8 (2008) 3856.
- [12] L.R. MacGillivray, *J. Org. Chem.* 73 (2008) 3311.
- [13] T. Lee, P.Y. Wang, *Cryst. Growth Des.* 10 (2010) 1419.
- [14] A.D.G.D. Mauro, M. Carotenuto, V. Venditto, V. Petraccone, M. Scoconi, G. Guerra, *Chem. Mater.* 19 (2007) 6041.
- [15] G.G. Hou, J.P. Ma, L. Wang, P. Wang, Y.B. Dong, R.Q. Huang, *Cryst. Eng. Commun.* 12 (2010) 4287.
- [16] D.P. Yan, A. Delori, G.O. Lloyd, T. Friščić, G.M. Day, W. Jones, J. Lu, M. Wei, D.G. Evans, X. Duan, *Angew. Chem. Int. Ed.* 50 (2011) 12483.
- [17] H.Y. Peng, C.K. Lam, T.C.W. Mak, Z.W. Cai, W.T. Ma, Y.X. Li, H.N.C. Wong, *J. Am. Chem. Soc.* 127 (2005) 9603.
- [18] I. Georgiev, E. Bosch, C.L. Barnes, M. Draganjac, *Cryst. Growth Des.* 4 (2004) 235.
- [19] C.L. Barnes, E. Bosch, *Cryst. Growth Des.* 4 (2005) 1049.
- [20] R. Horikoshi, C. Nambu, T. Mochida, *New. J. Chem.* 28 (2004) 26.
- [21] L. Brammer, *Chem. Soc. Rev.* 33 (2004) 476.
- [22] D.S. Zhou, F.K. Wang, S.Y. Yang, Z.X. Xie, R.B. Huang, *Cryst. Eng. Commun.* 11 (2009) 2548.
- [23] G.G. Hou, H.J. Zhao, J.F. Sun, D. Lin, X.P. Dai, J.T. Han, H. Zhao, *Cryst. Eng. Commun.* doi:10.1039/C2CE25759A.
- [24] Bruker. Analytical X-ray Systems, Inc., Madison, WI; 1998.
- [25] G.R. Desiraju, *Acc. Chem. Res.* 24 (1991) 290.
- [26] G.R. Desiraju, *Acc. Chem. Res.* 29 (1996) 441.
- [27] Y. Fan, Y.F. Zhao, L. Ye, B. Li, G.D. Yang, Y. Wang, *Cryst. Growth Des.* 9 (2009) 1421.
- [28] B. Kesanli, W. Lin, *Coord. Chem. Rev.* 246 (2003) 305.